

CHRISTIANE HELLING¹² RUPERT KLEIN
PETER WOITKE² ERWIN SEDLMAYR²

**Dust formation
in brown dwarf atmospheres
under conditions of driven turbulence³**

¹Zentrum für Astronomie und Astrophysik, TU Berlin, Hardenberstraße 36, 10623 Berlin,

²Guest member at ZIB

³Proceeding to the IAU-Symposium Nr. 210, 2002

Dust formation in brown dwarf atmospheres under conditions of driven turbulence

Christiane Helling Rupert Klein
Peter Woitke Erwin Sedlmayr

March 19, 2003

Abstract

Based on the knowledge gained from direct numerical simulations which are only possible in the microscale regime, a concept of driven turbulence is presented which allows to enter the mesoscopic scale regime. Here, dust formation under stochastic hydro- and thermodynamic conditions is studied: constructively superimposed stochastic waves initiate dust formation by the creation of singular nucleation events. It, hence, results a varying mean grain size and dust density in space and time. The newly formed dust changes the thermodynamic behavior from almost isotherm to adiabatic and chemically depletes the gas phase.

1 Introduction

Brown dwarfs have gained substantial interest during the last years not only due to their potential of physically bridging the gap between planets and stars but also as playground for the study of basic physics like dust formation and multi-scale phenomena like turbulence and convection.

Turbulence phenomena are characterized by an energy cascade from large to small scale until the energy is finally dissipated by the viscosity of the fluid. On the smallest scales, in the *microscopic* regime a direct numerical simulation of single turbulence events ('eddies') is feasible. Usually, this scale regime is modeled adopting some mean quantities in most of the turbulence simulations which, hence, do not allow a detailed investigation of the physics involved.

The microscopic regime provides a unique possibility to gain detailed insight into governing processes in a dust forming turbulent medium. The study of time-dependent dust formation under turbulent conditions in the *microscopic* scale regime ($l_{\text{ref}} \ll H_\rho$) has revealed a *feedback loop* in which interacting acoustic waves play the key role in initiating dust formation in otherwise dust-hostile environments. It results a highly variable distribution of dust in space and time (Helling et al. 2001). Based on the knowledge gained from the microscale investigations, we extent our studies to larger scales involving the Kolmogoroff inertial subrange. This presentation deals with the *mesoscopic* regime ($l_{\text{ref}} < H_\rho$) where *driven turbulence* is supposed to model a constantly occurring energy input from some convectively active zone outside a test volume.

2 Model of the reactive, dust forming gas flow

The physical and chemical processes in the reactive, dust forming gas in the brown dwarf atmosphere are described by the dimensionless hydrodynamical equations for mass, momentum and energy conservation (Eqs. 1–3) and the conservation equations for the chemistry and the dust complex (Eqs. 4, 5). The dust formation is thereby considered as a two-step process: formation of seed particles out of the gas phase (nucleation) and subsequent growth to macroscopic particles (Gail & Sedlmayr 1987, Dominik et al. 1990).

$$(\rho)_t + \nabla \cdot (\rho \mathbf{v}) = 0 \quad (1)$$

$$(\rho \mathbf{v})_t + \nabla \cdot (\rho \mathbf{v} \circ \mathbf{v}) = -\frac{1}{M^2} \nabla P - \gamma \frac{M^2}{Fr} \rho \mathbf{g} \quad (2)$$

$$(\rho e)_t + \nabla \cdot (\mathbf{v} [\rho e + P]) = Rd \kappa (T_{RE}^4 - T^4) \quad (3)$$

$$(\rho L_j)_t + \nabla \cdot (\mathbf{v} \rho L_j) = Da_d^{\text{nuc}} Se_j J_* + Da_d^{\text{gr}} \frac{j \chi^{\text{net}'} }{3} \rho L_{j-1} \quad (4)$$

$$(\rho \epsilon_x)_t + \nabla \cdot (\mathbf{v} \rho \epsilon_x) = - \sum_{r=1}^R (\nu_r^{\text{nuc}} El Da_d^{\text{nuc}} \sqrt[3]{36\pi} N_l J_* + \nu_r^{\text{gr}} El Da_d^{\text{gr}} n_{x,r} v_{\text{rel},x} \alpha_r \rho L_2) \quad (5)$$

All characteristic numbers and dimensionless quantities have the common meaning, and the others are:

| | | |
|---------------------|--|-----------------------------------|
| Rd | $= 4\kappa_{\text{ref}} \sigma T_{\text{ref}}^4 \cdot \frac{t_{\text{ref}}}{P_{\text{ref}}}$ | Radiation number |
| Da_d^{nuc} | $= \frac{t_{\text{ref}} J_{*,\text{ref}}}{\rho_{\text{ref}} L_{0,\text{ref}}}$ | Damköhler number of nucleation |
| Da_d^{gr} | $= \frac{t_{\text{ref}} \chi_{\text{ref}}}{(\frac{4\pi}{3} \langle a \rangle_{\text{ref}}^3)^{1/3}}$ | Damköhler number of growth |
| Se_j | $= \left(\frac{a_l}{\langle a \rangle_{\text{ref}}} \right)^j$ | Sedlmayr numbers (j = 0, 1, 2, 3) |
| El | $= \frac{\rho_{\text{ref}} L_{0,\text{ref}} N_l}{n_{<H>,\text{ref}} \epsilon_{\text{ref}}}$ | Element consumption number |

T_{RE} is the radiative equilibrium temperature, ϵ_x the element abundance of the chemical element x in mass fractions, L_j are the dust moments in mass fractions of the grain size distribution function $f(V)$ with V the single grain volume ($[L_j] = \text{cm}^j/\text{g}$), e is the total energy of the gas $\rho e = \gamma M^2 (\frac{\rho v^2}{2} + \frac{1}{Fr} \rho g y) + \frac{P}{\gamma-1}$, and g the gravitational acceleration acting in y direction.

The system of partial differential equations is closed by various material quantities which are partly expressed by non-linear algebraic equations (adiabatic coefficient γ , total absorption coefficient κ , rate of nucleation J_* , heterogeneous growth velocity χ_{net} ; for more details see Helling et al. 2001).

→ The analysis of the characteristic numbers shows that the *governing equations* of our model problem are those of an *inviscid, compressible fluid which are coupled to stiff dust moment equations and a singular radiative energy relaxation if dust is present.*

3 Stochastic boundary conditions driving turbulence

Turbulence is modeled by boundary conditions for our test volume: A disturbance $\delta\alpha(x, t)$ is added to a homogeneous background field $\alpha_0(x, t)$ such that for a suitable variable $\alpha(x, t) = \alpha_0(x, t) + \delta\alpha(x, t)$.

In order to fulfill the conservation equations inside the test volume, the stochastic, dust-free velocity, pressure and entropy fields are prescribed on ghost cells located outside the test volume. By solving the hydro-/thermodynamic equations (Eqs. 1-3), the stochastically created waves continuously enter the model volume and, thereby, a turbulent fluid field is generated.

The present pseudo-spectral model for driven turbulence comprises¹:

- **a stochastic distribution of velocity amplitudes $\delta\mathbf{v}(\mathbf{x}, \mathbf{t})$:**

$$e(k) = C_K \varepsilon^{2/3} k^{-5/3} \quad (6)$$

$$E_{\text{turb}}^i = \int_{k_{i+1}}^{k_i} e(k) dk = \frac{3}{2} C_K \varepsilon^{2/3} [k_i^{-2/3} - k_{i+1}^{-2/3}] \quad (7)$$

$$A_v(k_i) = \sqrt{2z_3 E_{\text{turb}}^i} \quad (8)$$

$$\delta\mathbf{v}(\mathbf{x}) = \sum_i A_v(k_i) \cos(k_i \hat{\mathbf{k}}_i \mathbf{x} + \omega_i \mathbf{t} + \varphi_i) \hat{\mathbf{k}}_i \quad (9)$$

The turbulent energy $E_{\text{turb}}^i = A_v(k_i)^2/2$ according to the Kolmogoroff spectrum is assumed to be the most likely value around which a stochastic fluctuation is generated by a Gaussian distributed number z_3 according to the Box-Müller formula $z_3 = \sqrt{-2 \log z_1} \sin(\pi z_2)$. z_1 and z_2 are equally distributed random numbers. The random numbers are chosen once at the beginning of the simulation. ε is the energy dissipation rate, $C_K = 1.5$ the Kolmogoroff constant, $k_i = |k_i \hat{\mathbf{k}}_i|$ are N equidistantly distributed wavenumbers in Fourier space ($i = 1, \dots, N$ with N the number of modes), and $\varphi_i = 2\pi z_4$ are the equally distributed random phase variations. From dimensional arguments the *dispersion relation* $\omega_i = (2\pi k_i^2 \varepsilon)^{1/3}$ was derived.

- **a stochastic distribution of pressure amplitudes $\delta P(\mathbf{x}, \mathbf{t})$:**

The pressure amplitude is determined depending on the wavenumber of the velocity amplitude $A_v(k_i)$ such that the compressible and the incompressible limits are matched for the smallest and the largest wavenumber:

$$A_P(k_i) = \frac{[k_{\text{max}} - k_i] \rho A_v(k_i)^2 + [k_i - k_{\text{min}}] \rho c_s A_v(k_i)}{[k_{\text{max}} - k_{\text{min}}]} \quad (10)$$

The Fourier cosine transform (as Eq. 9) provides $\delta P(\mathbf{x}, t)$ in ordinary space. $k_{\text{max}} = 2\pi/(3h)$ is the maximum wavenumber with h the spatial grid resolution, $k_{\text{min}} = 2\pi/l_{\text{ref}}$ is the minimum wavenumber with l_{ref} the size of test volume.

- **a stochastic distribution of the entropy $S(\mathbf{x}, \mathbf{t})$:**

The entropy $S(\mathbf{x}, t)$ is a purely thermodynamic quantity and a distribution can in principle be chosen independent on the distribution of the hydrodynamic

¹For examinations concerning the forcing in direct numerical simulations of turbulence see Eswaran & Pope (1988).

quantities. For a given entropy $S(\mathbf{x}, t)$ and given $P(\mathbf{x}, t)$ the gas temperature $T(\mathbf{x}, t)$ is given by:

$$\log T(\mathbf{x}, t) = \frac{S(\mathbf{x}, t) + R \log P(\mathbf{x}, t) - R \log R}{c_V + R} \quad (11)$$

So far, $S(\mathbf{x}, t)$ has been kept constant. R is the ideal gas constant, $c_V = 3k/(2\mu)$ the specific heat capacity ($V = \text{const}$) for an ideal gas, k the Boltzmann constant, and $\mu = 2.3 m_H$ the mean molecular weight.

4 Numerical features

A full time-dependent solution of the model equations (1–5) has been obtained by applying a multi-dimensional Euler solver for compressible fluids (Smiljanovski et al. 1997) which has been extended to treat consistently the complex of dust formation, radiative cooling and element consumption. The simulations have been performed with a spatial resolution of 500 grid points. The **initial conditions** are chosen to be dust free and homogeneous hydrodynamic, thermodynamic and dust quantities have been adopted: $L_0(\mathbf{x}, 0) = 0$, $P(\mathbf{x}, 0) = \rho(\mathbf{x}, 0) = S(\mathbf{x}, 0) = \text{const}$, $\mathbf{v}(\mathbf{x}, 0) = 0$. The **boundary conditions** are modeled as described in Sect. 3.

A strong feedback between dust and radiative cooling occurs due to the large opacity of the dust and its strong temperature sensitivity. Considerable numerical difficulties result. Therefore, the coupled dust and radiative cooling complex is solved by the LIMEX DAE solver for each hydrodynamic time step with adaptive time-step control (Deuffhard & Nowak 1987). In contrast to the CVODE solver, LIMEX does not fail to solve the transition from a dynamic to an equilibrium situation of the dust complex (Eqs. 4, 5) which is strongly coupled to the radiative source term of Eq. (3).

5 Results

The simulations presented here are first calculations for a typically hot and dense, dust-hostile region in an atmosphere of a brown dwarf star in the mesoscopic regime *applying a concept of driven turbulence*. If appropriate thermodynamic conditions occur, dust particles are formed out of the gas phase; considered are TiO_2 -seeds on which SiO and TiO_2 grow via surface reactions.

The simulations are characterized by a set of reference values from which a set of characteristic numbers results. The hydrodynamic, thermodynamic and dust values (Eqs. 1–5) will evolve during the simulation and can thereby considerably diverge from the reference values which are:

reference values:

| | | |
|--|--|--|
| $T_{\text{ref}} = 2100 \text{ K}$ | $v_{\text{ref}} = c_s/10$ | $J_{*,\text{ref}} = 10^{14} \text{ 1/(s cm}^3\text{)}$ |
| $\rho_{\text{ref}} = 10^{-4} \text{ g/cm}^3$ | $c_s = 4 \cdot 10^5 \text{ cm/s}$ | $L_{0,\text{ref}} = 10^{10} \text{ 1/g}$ |
| $P_{\text{ref}} = 10^7 \text{ dyn/cm}^2$ | $g_{\text{ref}} = 10^5 \text{ cm/s}^2$ | $\chi_{\text{ref}} = 10^{-2} \text{ cm/s}$ |
| $S_{\text{ref}} = 10^9 \text{ erg/K}$ | $l_{\text{ref}} = 10^5 \text{ cm}$ | $\langle a \rangle_{\text{ref}} = 10^{-6} \text{ cm}$ |
| $\kappa_{\text{ref}} = 10^{-2} \text{ cm}^2/\text{g}$ | $T_{\text{RE}} = 1900 \text{ K}$ | $\epsilon_{\text{ref}} = 10^{-6}$ |
| $\Rightarrow \epsilon_{\text{ref}} = 10^8 \text{ cm}^2/\text{s}^3$ | $t_{\text{ref}} = 2.5 \text{ s}$ | |

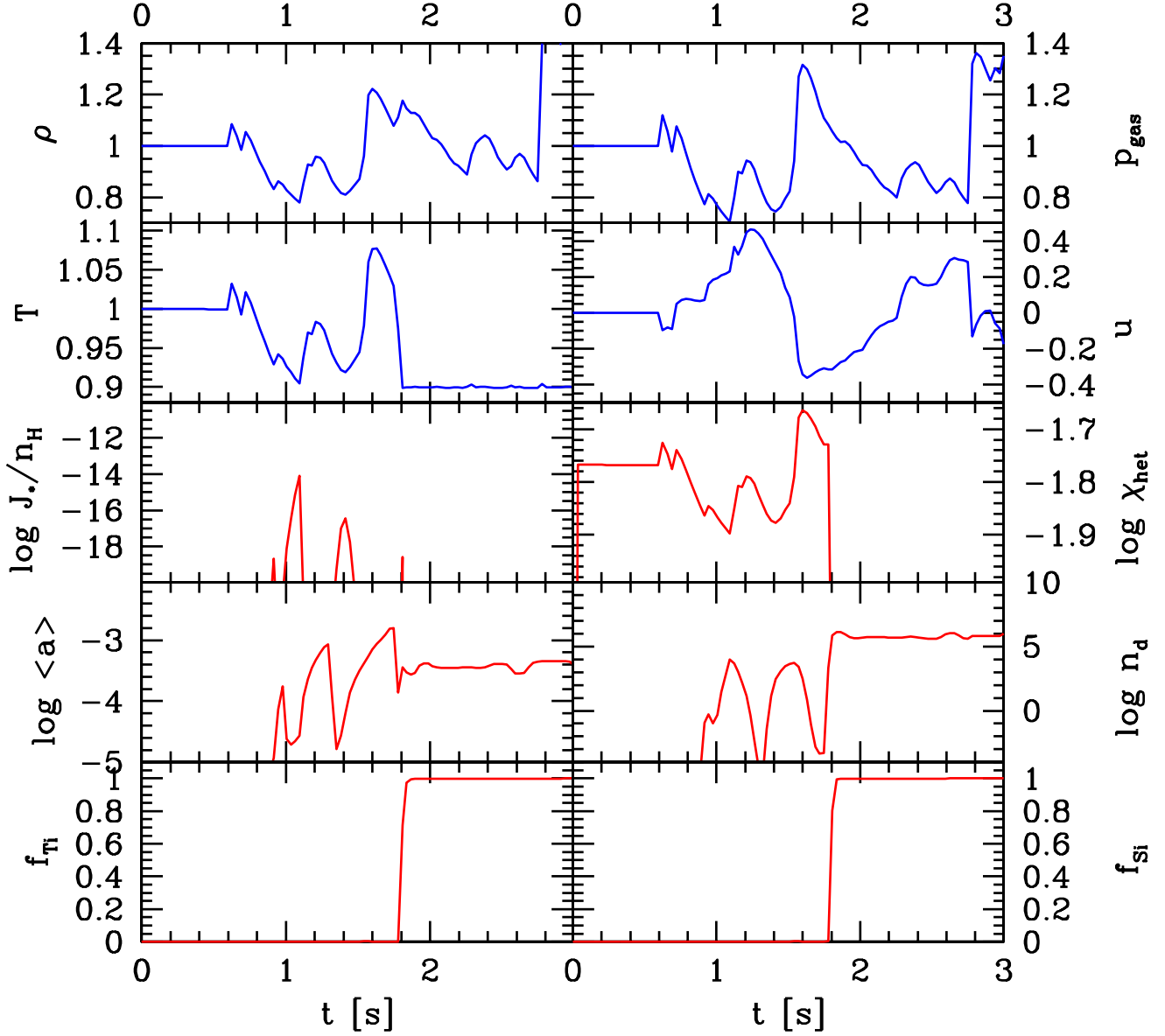


Figure 1: The time evolution of hydrodynamic (blue) and dust (red) quantities at the center of the test volume ($x = 0.25 l_{\text{ref}}$) for a turbulent gas driven by 50 k -modes.

(ρ - gas density, p - gas pressure, T - gas temperature, u - hydrodynamic velocity (dimensionless); $J_*/n_{\langle H \rangle}$ - nucleation rate [1/s], χ_{net} - net growth velocity [cm/s], n_d - number of dust particle [1/cm³], $\langle a \rangle$ - mean particle radius [cm], f_{Ti} - degree of consumption of Ti, f_{Si} - degree of consumption of Si).

characteristic numbers:

| | | | | | |
|-------------|-------------|----|--------|--------------------------------|---------------------|
| Rd | = 10^{-2} | M | = 0.1 | Da _d ^{nuc} | = $2.5 \cdot 10^8$ |
| (dust free) | | Fr | = 0.16 | Da _d ^{gr} | = $1.5 \cdot 10^4$ |
| | | | | Se _j | = $1 \dots 10^{-2}$ |
| | | | | El | = 10^{-2} |

The large values of the characteristic dust Damköhler numbers, Da, indicate the dominance of the dust formation process if appropriate conditions occur. The radiation number, Rd, will increase by order of magnitudes if dust has formed which causes also the radiative cooling to be one of the dominating processes inside the dust formation window.

→ **Remark:** Characteristic numbers are not unique. Therefore, each solution (e.g. Fig. 1) of the model Eqs. (1–5) represent *a whole family of solutions* concerning different reference values for one set of characteristic numbers as e.g. given above.

Figure 1 depicts the results of our 1D simulation with stochastic boundary conditions. The time evolution of hydrodynamic, thermodynamic, and dust quantities in the center of the test volume are shown.

Two evolutionary epochs can be distinguished:

1) pre-RE epoch:

Interacting stochastic waves provide locally low enough temperatures that nucleation is possible for a short time interval (*singular nucleation events*). Subsequent dust growth causes the dust particle mean size $\langle a \rangle$ to increase. T reaches the radiative equilibrium (RE) level due to the resulting increase of the absorption coefficient κ .

During this epoch, $\langle a \rangle$ and n_d vary considerably until $f_{Ti} = f_{Si} = 1$, consequently the supersaturation ratio $S < 1$, and the dust complex has reached a steady state.

2) past-RE epoch:

The stochastically created waves can not any more alter the temperature since the dust immediately drives the temperature back to the RE level. All condensable material has been consumed by the dust, hence, $S < 1$ and the dust complex can not change further. Only the already existing dust particles in the test volume are transported by the incoming stochastically superimposed waves.

In the long run, the dust complex is characterized by small fluctuation in the mean particles size $\langle a \rangle$ ($\log \langle a \rangle \approx -3.5 \pm 0.25$) and number density n_d ($\log n_d \approx 6 \pm 1$) after the dust has reached its steady state where the gas is undersaturated. The dust is considerably more inhomogeneous in mean size and density close to the boundary where the stochastic waves enter the test volume compared to the center of the test volume discussed here.

6 Conclusions

- The dust formation is initiated by the constructively superimposed stochastic waves resulting in a varying mean grain size and dust density in space and time.
- The dust changes the thermodynamic behavior from almost isotherm to adiabatic and chemically depletes the gas phase during the **pre-RE epoch**. An pure temperature increase extends this phase.
- The dust drives the temperature always back into radiation equilibrium due to its large opacity during the **past-RE epoch**.

Acknowledgment Dr. U. Nowak (ZIB) is thanked for the support in implementation and application of LIMEX, Dipl.-Ing. H. Schmidt for discussions on the poster's topic. This work has been supported by the DFG (grants Se 420/19-1, Se 420/19-2, Kl 611/8-1 and SFB 555 Teilprojekt B8).

References

- Deuffhard P., Nowak U., 1987, In Deuffhard P., Engquist B., Large Scale Scientific Computing. Progress in Scientific Computing, 7, 37–50. Birkhäuser
- Dominik C., Gail H.-P., Sedlmayr E., Winters J. M., 1990, A&A, 240, 365
- Eswaran V., Pope S.B., 1988, Computers & Fluids, 16/3, 257
- Gail H.-P., Sedlmayr E., 1987, A&A, 171, 197
- Helling Ch., Oevermann M., Lüttke M., Klein R., Sedlmayr E., 2001, A&A, 376, 194
- Smiljanovski V., Moser V., Klein R., 1997, Combustion Theory & Modelling, 1, 183